

Life at the edge of methane ice: microbial cycling of carbon and sulfur in Gulf of Mexico gas hydrates

Beth N. Orcutt^a, Antje Boetius^{b,c,d}, Samantha K. Lugo^a, Ian R. MacDonald^e,
Vladimir A. Samarkin^a, Samantha B. Joye^{a,f,*}

^aDepartment of Marine Sciences, University of Georgia, Athens, GA 30602, USA

^bAlfred Wegener Institute for Polar and Marine Research, 27515 Bremerhaven, Germany

^cMax Planck Institute for Marine Microbiology, 28359 Bremen, Germany

^dInternational University Bremen, 28759 Bremen, Germany

^eDepartment of Physical and Life Sciences, Texas A&M University, Corpus Christi, TX 78412, USA

^fHanse Institute for Advanced Study, 27753 Delmenhorst, Germany

Received 3 December 2002; received in revised form 28 April 2003; accepted 23 December 2003

Abstract

The processes of methane oxidation and sulfate reduction were examined in subsamples of gas hydrate associated materials collected along the Gulf of Mexico continental slope. Standard radiotracer techniques were used to determine rates of microbial activity in different layers of the hydrate environment, including outer sediment (OS), interface sediment (IS), worm burrow sediment (WB), interior hydrate (IN) and a mixture of hydrate and sediment (MIX). The anaerobic oxidation of methane (AOM) and sulfate reduction (SR) were observed in all hydrate samples examined and the rates of these processes showed similar spatial trends between different hydrate layers. Highest rates of both AOM and SR were observed at interface between the sediment and hydrate. AOM rates were about 3–11 nmol cm⁻³ day⁻¹ in worm burrow and interface sediments as compared to <1 nmol cm⁻³ day⁻¹ in other hydrate material types. Rates of SR ranged from 59 to 490 nmol cm⁻³ day⁻¹ in worm burrow and interface sediments while rates in interior hydrate samples were an order of magnitude lower. These rates observed in hydrate materials are lower than rates from nearby methane-rich sediments at ambient temperatures. Nevertheless, our data show that active microbial populations inhabit all layers of the hydrate environment and suggest their activity may impact biogeochemical methane and sulfur cycling in this unique niche.

© 2004 Elsevier B.V. All rights reserved.

Keywords: Anaerobic oxidation of methane; Sulfate reduction; Gas hydrates; Gulf of Mexico

1. Introduction

Gas hydrates represent one of the largest and most dynamic reservoirs of organic carbon, in particular methane, on Earth (Kvenvolden, 1993; Collett and Kuuskraa, 1998). Current estimates of the mass of carbon in global gas hydrate vary; however, the

* Corresponding author. Department of Marine Sciences, University of Georgia, Room 220, Marine Sciences Building, Athens, GA 30602, USA. Tel.: +1-706-542-7671; fax: +1-706-542-5888.

E-mail address: mjoye@arches.uga.edu (S.B. Joye).

reservoir mass is probably between 10^{18} and 10^{19} g of carbon (Kvenvolden, 1988; Collett and Kuuskraa, 1998; Dickens, 2001). Data from geochemical models, paleontological analyses and stable carbon isotopes suggest that large changes in global hydrate inventories have contributed to rapid shifts in global climate in past periods of Earth history (Dickens et al., 1995; Norris and Röhl, 1999; Kennett et al., 2000;

Hesselbo et al., 2000). The largest fraction of the gas hydrate reservoir is buried beneath 200–300 m of sediment at the base of continental margins (Kvenvolden, 1993), where rates of methane oxidation may be presumed to be slow (Hoehler et al., 2000). Gas hydrate deposits may also occur in the upper few meters of seafloor sediments (Brooks et al., 1991, 1984; Ginsburg et al., 1992, 1999; MacDonald et al.,

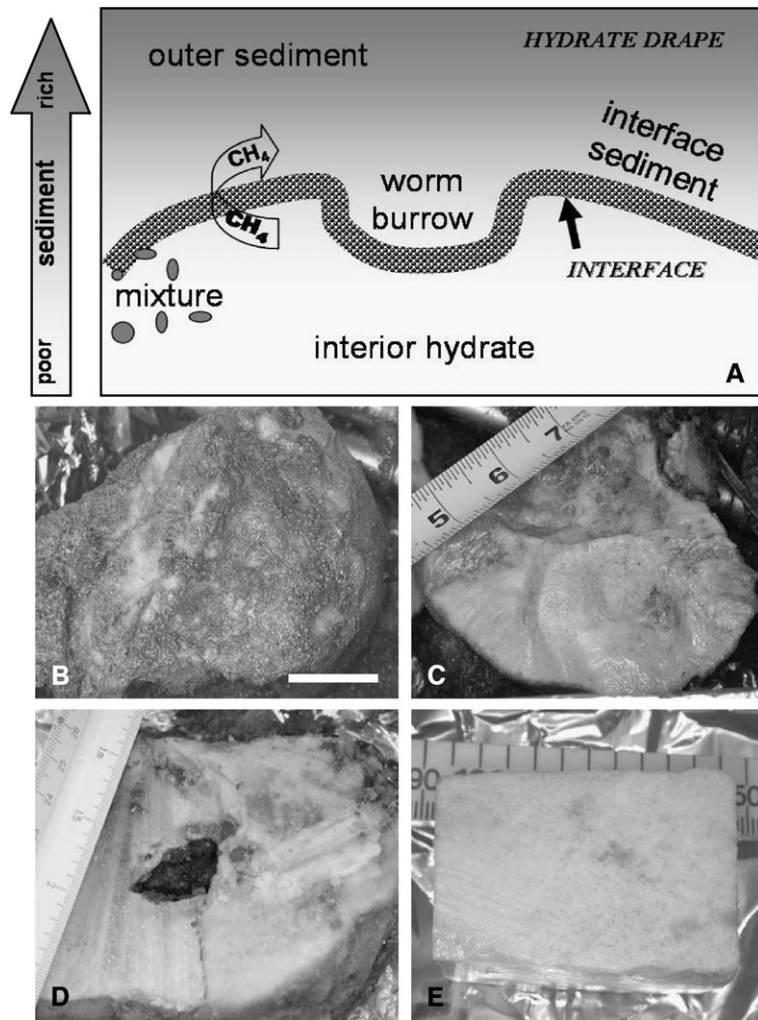


Fig. 1. Cartoon showing the layering of Gulf of Mexico gas hydrate used in these experiments. (A) Diagram depicting different layers, arrow on left indicates relative sediment content. Patterned line through diagram represents the sediment/hydrate interface, where high methane conditions result from hydrate dissolution. Lower case labels indicate the location of samples described in the text. (B) Photo of recovered gas hydrate after outer sediment layer has been removed. Scale bar ~ 1 in. (C) Cross-section through sample shown in (B), dark areas are entrapped sediment and oily material; ruler (in inches) for scale. (D) Photo of “MIX” layer showing sediment entombed within the hydrate; ruler (in cm and inches) for scale. (E) “Interior hydrate” sample, darker areas represent oily material; ruler (0.5 cm gradations) for scale. (Photo credits: I. R. MacDonald).

1994). In these settings, particularly when a hydrate deposit is exposed to seawater or covered by a thin drape of sediment, methane oxidation, dissolution of hydrate gases into seawater, and microbial alterations of gas hydrate would be expected to be much more active.

On a global scale, the aerobic and anaerobic microbial oxidation of methane is estimated to consume 80–90% of the methane produced by natural and anthropogenic sources annually (Reeburgh et al., 1993; Reeburgh 1996). However, rates of methane oxidation in hydrate environments are poorly documented (Hinrichs and Boetius, 2002). Microbial methane oxidation functions like a barrier in consuming upwardly diffusing hydrate-derived methane in the overlying sediments (Hoehler et al., 2000) and in the overlying water column (Valentine et al., 2001). Methane oxidation could thus ameliorate or buffer climate impacts resulting from slow hydrate dissociation. Rapid destabilization of hydrate may result in gas bubbling and floating of hydrates and is most likely not controlled by microbial methane oxidation. However, microbial consumption in and around hydrate affects hydrate stability, which depends not only on temperature and pressure, but also on methane concentration in the vicinity of hydrates. Sediment methane oxidation effectively sequesters hydrate carbon in the form of carbonates over longer time scales (Sassen and MacDonald, 1994; Whiticar, 1996; Michaelis et al., 2002) while water column oxidation may aid in sequestering methane-derived carbon in the planktonic food web as organic or inorganic carbon (Kennett et al., 2000).

In marine sediments, microbial anaerobic oxidation of methane (AOM) and sulfate reduction (SR) proliferates near the methane–sulfate interface, where supplies of oxidant (sulfate, SO_4^{2-}) and reductant (methane, CH_4) are concurrently available. AOM and SR are hypothesized to be coupled in anoxic environments according to the following net reaction (Reeburgh, 1980; Hoehler et al., 1994):



This coupling between AOM and SR has been documented in other methane-rich sediments using enrichment and radiotracer methods (Nauhaus et al., 2002; Michaelis et al., 2002).

To evaluate the activity of microorganisms in hydrates and hydrate-draping sediment, we obtained samples of intact hydrate and associated sediments and determined the magnitude and spatial distribution of AOM and SR using radiotracer methods. We hypothesized that rates of these processes would vary between different layers of the hydrate environment (outer sediment (OS), interface sediment (IS), sediment accumulated in hydrate worm burrows (WB), interior hydrate (IN), and a mixture of interface sediment and hydrate (MIX), see Section 2.1 and Fig. 1) due to geochemical and physical differences between the layers. These novel studies indicate that spatial heterogeneity in both processes exists in the hydrate environments. Due to the presence of many other types of hydrocarbons in the hydrate environments in the Gulf of Mexico, which might also be used as microbial substrates, it is difficult to discern definitively whether AOM and SR are stoichiometrically coupled.

2. Materials and methods

2.1. Site description

Samples of solid hydrate and hydrate-draping sediment (Fig. 2) were collected during July 2001 and July 2002 from two sites (GC 234 and GC 232) along the continental slope in the northern Gulf of



Fig. 2. An underwater photo of a surface-breaching hydrate. Arrows indicate worm burrows in the hydrate surface, and a *Beggiatoa* mat is present (labeled) at the lower left. (Photo credit: I.R. MacDonald).

Mexico (see Joye et al., submitted for publication, Fig. 1, for detailed map). Natural gas and oil continuously seep from the seafloor at these sites (Kennicutt et al., 1988; MacDonald et al., 1994) and near- or surface-breaching hydrates exist on the edge of the hydrate stability curve between 500 and 700 m (5–7 MPa) and 7–8 °C. Gulf of Mexico hydrates occur as Structure II, being comprised of methane (70–85%) and higher alkanes (Brooks et al., 1984; Sassen and MacDonald, 1994; Sassen et al., 1999). Sediments around hydrates were predominantly clay-rich silts. At these sites, methane serves as the base of a complex chemosynthetic ecosystem by supporting both free-living and symbiotic bacteria (MacDonald et al., 1989, 1994). Hydrate deposits are often evident as prominent topographic mounds that can be several meters in height and up to 10 m in diameter (MacDonald et al., 2003). The mounds comprise displaced sediments, as well as solid hydrate, and are colonized by chemosynthetic species of tube worms and mussels. Mats of giant sulfide-oxidizing bacteria cover exposed hydrate mounds, creating a living interface between the overlying water, nearby anoxic sediments and the solid hydrate surface. Polychaete “ice” worms (*Hesiocaeca methanicola*) create burrows in the hydrate surface and in the sediment drape; burrows in the interior of the hydrate may subsequently fill with sediment (Fig. 2; Fisher et al., 2000).

2.2. Sample collection

Samples of hydrate material were collected during multiple dives of the Johnson Sea-Link submersible operated by the R/V Seward Johnson I and II (Harbor Branch Oceanographic Institute, Fort Pierce, FL). A hydrate “chipper” operated by the robot arm of the submersible removed contiguous sections of hydrate and the surrounding hydrate-drape sediments from hydrate mounds exposed at the seafloor. The sample material was placed into an insulated pressure-retaining hydrate recovery chamber. The hydrate chamber contained ambient bottom water. After collection, the chamber was sealed with a pressure-retaining lid equipped with a vent valve, which prevented significant over pressure within the chamber. The chamber is insulated with low-density plastic to prevent heat gain during recovery through

warm surface waters; consequently, the chamber assured delivery of intact hydrate/sediment material to the surface with minimum degassing. Upon retrieval, the hydrate chamber was transferred quickly to a cold laboratory (8 °C in 2001, 4 °C in 2002) for processing.

Intact sections of hydrate and sediment material in the hydrate chamber were removed and placed in a liquid nitrogen-chilled sterile tub for sectioning with sterile instruments (Fig. 1). The outer 1–3 mm of material in contact with seawater in the hydrate collection chamber was carefully pared away to remove potentially contaminated material. Next, the following layers were separated using sterile instruments and were placed into separate sterile containers (150 ml I-chem® jars): outer sediment (OS): sediment more than a centimeter away from the hydrate surface; interface sediment (IS): sediments directly in contact with the hydrate; worm burrow sediment (WB): sediment from inside a worm burrow on the hydrate surface; interior hydrate (IN): solid hydrate more than 5 cm from the surface that contained minimal (if any) sediment debris; and a mixture of sediment and hydrate chunks (MIX): outer hydrate layer co-mingled with sediment material that was “frozen” into the hydrate matrix (Fig. 1). Samples from each layer were separated and transferred quickly to Ar-purged sterile glass I-chem® vials sealed with a Teflon-lined septa screw cap. Solid hydrate slowly sublimed in the vials at ambient surface pressure. Vial over pressure was relieved by inserting a vent needle into the septa or through sampling (see Section 2.3). Samples remained at 8 °C during manipulation and until subsequent processing. Results presented here represent data conducted from multiple hydrate collections at each study site.

In both years, vent gas escaping near hydrates was collected to compare the vent gas C₁–C₅ hydrocarbon composition to the hydrate C₁–C₅ hydrocarbon composition. Comparison of the molecular ratios of vent gas and solid hydrate allows evaluation of hydrate structure and may help elucidate microbial alteration of hydrate gases. Vent gas was collected into an inverted butyrate tube that was open at the bottom and sealed with a gas tight lid equipped with a sampling port. The tube, which was initially filled with water, was held over a stream of bubbles, which

displaced the water and collecting into the tube. Upon surfacing of the submersible, gas samples were collected into He-purged, evacuated, crimp-sealed headspace vials.

2.3. Geochemical measurements

To determine the molecular composition of hydrate samples, material was sectioned and stored as described above. When the hydrate sample began to sublime and degas, a vent needle was used to puncture the Teflon-lined sampling port. A gas volume of at least 200-ml vented from the jar and then a subsample of headspace gas was transferred from each vial into a He-flushed 60-cc plastic syringe. This subsample was stored in replicate He-purged, evacuated 20-ml headspace vials that were crimp-sealed with butyl rubber stoppers. Concentrations of C₁–C₅ hydrocarbons in hydrate and vent gas samples were determined on-board ship using a gas chromatograph (Shimadzu 14-A) equipped with a flame-ionization-detector. Individual gases were separated on a Haysep[®] DB column (100/120 mesh) by application of a temperature ramp. Peaks were quantified by comparison with a certified C₁–C₅ gas standard (Joye et al., 2004).

For the determination of major ions, subsamples of hydrate material were transferred from the chilled tub into crimp-sealed, Ar-flushed headspace vials. The samples sublimed and the melt fluid was separated from particulate material by centrifugation. Supernatant was withdrawn into a sterile plastic syringe, and a filtered (0.2- μ m acrodisc[®]) 0.5–1.0-ml aliquot was fixed with 100 μ l of 50% H₃PO₄ or conc. HNO₃ in an Ar-flushed vial. Samples were stored at 4 °C until analysis. Sulfate and chloride concentrations were determined by ion-chromatography (Dionex[®]) in comparison with both certified and lab standards (Joye et al., 2004). Concentration values are reported as the average of multiple ($n > 3$) analyses conducted on separate hydrate samples from the same site.

2.4. Bacterial counts

Subsamples of hydrate material were preserved by formaldehyde fixation for determination of microbial cell numbers using acridine orange direct

counting (AODC, Hobbie et al., 1977). The AODC method was chosen because it does not suffer from interference due to oil fluorescence, which is common in these hydrate samples, and which may have caused difficulties in cell identification in previous studies where a different method (e.g. DAPI) was used (Lanoil et al., 2001).

2.5. Methane oxidation rates

Rates of AOM in hydrate material were determined using a ¹⁴CH₄ tracer technique (Joye et al., 1999, 2004). Aliquots of material from specific hydrate layers were rapidly transferred under a stream of argon (to keep samples anoxic) from collection vials into either (1) Ar-flushed 8.5-ml headspace vials crimp-sealed with butyl rubber stoppers or (2) glass tubes sealed at one end with a plunger and at the other with a rubber stopper. Hydrate material in serum vials was slurried by filling bottles with sterile filtered (0.2 μ m), UHP CH₄/Ar (10/90) purged bottom water ([CH₄]=130 μ M, [SO₄²⁻]=28 mM). Each sample set included two to four replicates of each treatment depending on amount of material available. At least one control, which was fixed immediately after isotope addition, was included with each sample set. 30–60 μ l of dissolved ¹⁴CH₄ tracer (activity 1500 dpm μ l⁻¹ or \sim 0.68 nCi μ l⁻¹, dissolved in sterile, anoxic Milli-Q[®] water) was added to samples using a gas-tight syringe. Samples were incubated in the dark at 8 °C for 24–48 h. Experiments were terminated by replacing 1 ml of the slurry volume with 1 ml of anoxic 1 N NaOH (to stop biological activity and fix generated ¹⁴CO₂ as bicarbonate). The displaced 1 ml of sample fluid was preserved in a 7-ml scint vial containing 1 ml anoxic 1 N NaOH. All samples were stored at 4 °C until analysis. For syringe incubations, experiment were terminated by transferring the sediment volume into a 20-ml glass vial containing 3 ml of 1 N NaOH and sealing the vial with a Teflon-lined screw cap. The activities of ¹⁴CH₄ and ¹⁴CO₂ and the rate of AOM (nmol cm⁻³ day⁻¹) were determined using previously described methods (Joye et al., 1999, 2004). Rates presented here were normalized to the original sample volume and are averages of replicate collections at each site.

2.6. Sulfate reduction rates

Sulfate reduction (SR) rates were determined using ^{35}S -techniques (Canfield et al., 1986; Fossing and Jørgensen, 1989). In 2001, samples were slurried in the same way as AOM samples (see above). In 2002, additional samples were prepared without slurring to evaluate SR rates at in situ SO_4^{2-} concentrations. Non-slurry samples were prepared in glass tubes sealed at both ends with butyl rubber stoppers. Thirty to sixty microliters of carrier-free $^{35}\text{SO}_4$ tracer (activity 88000 dpm μl^{-1} or ~ 40 nCi μl^{-1} , dissolved in sterile, anoxic Milli-Q[®] water) was added to the samples using a gas-tight syringe. Samples were incubated in the dark at 8 °C for 24–48 h. Experiments were terminated by transferring each sample into 50-ml centrifuge tubes (15 ml in 2001) containing 10 ml (7 ml in 2001) of 20% zinc acetate (ZnAc; to stop biological activity and preserve reduced ^{35}S -sulfide as Zn ^{35}S). Samples were stored frozen until analysis on-shore. The radioactivity of SO_4^{2-} (the substrate) was determined by counting an aqueous subsample of the fixation solution after centrifugation and the radioactivity of H_2S (the product) was determined using a one-step hot chromous acid digestion. The SR rate (nmol cm^{-3} day^{-1}) was calculated using a published rate equation (Canfield et al., 1986; Fossing and Jørgensen, 1989; Joye et al., 2004) and normalized to original sample volume; values presented represent an average from replicate collections of hydrate material at a given site (as for AOM).

3. Results

3.1. Geochemistry

During the hydrate crystallization, certain gases are concentrated in the matrix resulting in differences between the source gas molecular composition and the hydrate molecular composition (Sloan, 1990). As expected, ratios of hydrocarbon gases varied between vent gas and sublimed hydrate at GC232 and at GC234 (Table 1). Enrichment of $>\text{C}_2$ alkanes (e.g. ethane and propane) was observed at both sites, as expected for structure II hydrate. The GC232 vent gas was approximately 91% methane,

Table 1

The percentage composition of C_1 to C_5 hydrocarbons in hydrate material and vent gas from sites GC232 and GC234

Hydrocarbons	Vent gas	Interior	Edge
<i>GC232</i>			
Number of samples	3	7	3
Percentage	%	%	%
Methane (C_1)	90.7 (0.1)	49.8 (1.5)	49.9 (5.5)
Ethane (C_2)	5.2 (0.1)	15.9 (1.7)	18.2 (7.2)
Propane (C_3)	1.1 (0.1)	25.1 (2.2)	22.3 (0.3)
<i>iso</i> -Butane (<i>iso</i> - C_4)	0.1 (0.02)	6.1 (1.1)	4.7 (1.2)
Butane (C_4)	1.4 (0.2)	2.8 (0.6)	4.5 (0.9)
Pentane (C_5)	1.4 (0.1)	0.3 (0.3)	0.5 (0.1)
<i>GC234</i>			
Number of samples	5	6	4
Percentage	%	%	%
Methane (C_1)	86.5 (0.2)	44.4 (4.7)	40.3 (1.6)
Ethane (C_2)	6.9 (0.1)	12.1 (4.6)	9.3 (0.8)
Propane (C_3)	4.2 (0.1)	26.8 (11.3)	36.4 (1.7)
<i>iso</i> -Butane (<i>iso</i> - C_4)	0.6 (0.02)	8.4 (2.3)	11.2 (1.0)
Butane (C_4)	1.5 (0.01)	2.8 (0.6)	2.3 (0.4)
Pentane (C_5)	0.2 (0.01)	0.3 (0.1)	0.5 (0.01)

The average value and the standard deviation of the mean (in parentheses) are shown.

whereas the GC232 hydrate was about 50% methane and a large fraction of ethane and propane. Compared to the GC232 vent gas, the GC234 vent gas contained less methane and more ethane and propane (Table 1). The GC234 hydrate material was similar in composition to the GC232 hydrate, however, the edge hydrate material and interior hydrate material exhibited slight differences in the percent methane (4% lower at the edge than in the interior).

Multiple analyses of hydrate and sediment material illustrated variable concentrations of major anions. Sulfate (SO_4^{2-}) and chloride (Cl^-) concentrations differed between hydrate layers (Table 2). The lowest SO_4^{2-} concentrations were observed in sediment-free IN (3.5 to 4 mM). The MIX samples exhibited a range of SO_4^{2-} values (5 to 9.5 mM). The WB sediment had the highest SO_4^{2-} concentration at 17.9 mM. The IS contained varying amounts of SO_4^{2-} , ranging from 5.5 to 12.4 mM. The OS averaged about 11.5 mM SO_4^{2-} . Similarly, Cl^- concentrations were lowest (~ 150 mM) in IN material and highest (~ 450 mM) in WB material. The Cl^- concentrations in the OS material averaged about 390 mM, in the MIX about 300 mM, and in

Table 2

Rates of AOM and SR in gas hydrate material collected from two sites in the Gulf of Mexico

Hydrate sample	Code	AOM (nmol cm ⁻³ day ⁻¹)	SR (nmol cm ⁻³ day ⁻¹)	SO ₄ ²⁻ (mM)	Cl ⁻ (mM)
<i>GC234 in 2001</i>					
Outer sediment	OS	0.3 (0.1)	100 (82)	11.0 ^a	382.9
Interface sediment	IS	11 (1.9)	489 (76.2)	12.4	401.7
Mixture	MIX	0.75 (0.42)	118 (58)	4.9	338.2
Interior hydrate	IN	0.72 (0.66)	54.7 (36.6)	3.5	137.1
<i>GC234 in 2002</i>					
Outer sediment	OS	0.60 (0.2)	76.2 (20.8)	12.3 (1.4)	397.2 (158.2)
Interface sediment	IS	3.25 (1.7)	n.d. ^b	5.5 (0.3)	231.1 (115.9)
Worm burrow sediment	WB	2.43 (0.3)	n.d.	n.d.	n.d.
Mixture	MIX	0.13 (0.1)	23.0 (1.0)	9.5 (1.0)	317.0 (111.0)
Interior hydrate	IN	0.28 (0.3)	3.2 (4.1)	3.2 (2.1)	150.0 (142.4)
<i>GC232 in 2002</i>					
Worm burrow sediment	WB	10.74 (0.2)	59.0 (7.8)	17.9 ^c	451.4
Mixture	MIX	0.74 (0.04)	18.8 (2.3)	6.6	285.8
Interior hydrate	IN	0.36 (0.5)	0.6 (0.1)	4.0 (1.9)	158.5 (19.8)

Data is grouped by year, site and material type. Rates (nmol cm⁻³ day⁻¹) represent the average of replicates ($n > 3$) from multiple collections and standard deviation of the mean is shown in parentheses. Average sulfate and chloride concentrations of original hydrate material are also shown (mean standard deviation in parentheses).

^a No replicates available for sulfate and chloride concentrations in 2001.

^b Not determined.

^c No replicates available for major ions.

the IS material from 230 to 400 mM., The SO₄/Cl ratio ranged between 0.02 and 0.04, which is less than the value (0.05) expected for seawater, suggesting some SO₄ consumption occurs under natural conditions.

3.2. Bacterial numbers

In both years, hydrate-drape sediment material had higher cell counts than the interior hydrate material. Hydrate-drape material (OS, IS, and WB) contained an average of 1×10^9 cells cm⁻³, while MIX material and IN had averages of $4\text{--}7 \times 10^8$ and $2\text{--}5 \times 10^7$ cells cm⁻³, respectively. The hydrate-drape sediment material contained a variety of microbial morphotypes; a large fraction was rod-shaped, usually as double rods or in rod chains, similar to the morphologies described for ANME1 archaea (Orphan et al., 2001, 2002; Fig. 3A). The morphology of interior hydrate microorganisms was dominated by such rod-shaped cells, usually occurring as double rod chains (Fig. 3B).

3.3. Methane oxidation rates

Anaerobic oxidation of methane was observed in all layers of hydrate but rates varied between layers (Table 2, Fig. 4). Highest AOM rates were observed in sediment material from the hydrate interface (i.e. worm burrow and interface sediment). In GC234 samples in 2001 (slurried), the IS exhibited the highest AOM rates ($11.2 \text{ nmol cm}^{-3} \text{ day}^{-1}$), an order of magnitude greater than rates observed in the other layers. Similarly, in 2002, the highest AOM rates were observed in material from the interface of the hydrate ($2.4\text{--}3.3 \text{ nmol cm}^{-3} \text{ day}^{-1}$ in WB and IS, respectively). Rates at the interface exceeded activity observed in the sediment-poor hydrate material (MIX and IN: 0.1 and $0.3 \text{ nmol cm}^{-3} \text{ day}^{-1}$, respectively) and in outer sediments (OS: $0.6 \text{ nmol cm}^{-3} \text{ day}^{-1}$). Hydrate samples from GC 232 displayed a similar distribution of rates: $10.7 \text{ nmol cm}^{-3} \text{ day}^{-1}$ in WB and $\leq 0.7 \text{ nmol cm}^{-3} \text{ day}^{-1}$ in MIX and IN. Significant variability in rates of AOM between replicate samples was observed in both years (Table

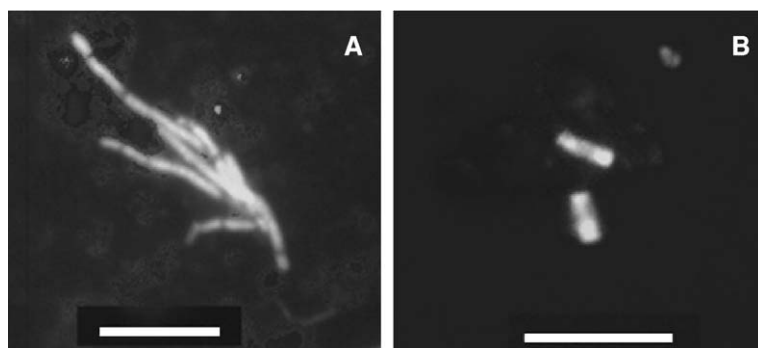


Fig. 3. Microscopic images of hydrate-associated microorganisms stained with acridine orange from (A) interface sediment and (B) interior hydrate. Scale bar is 5 μm .

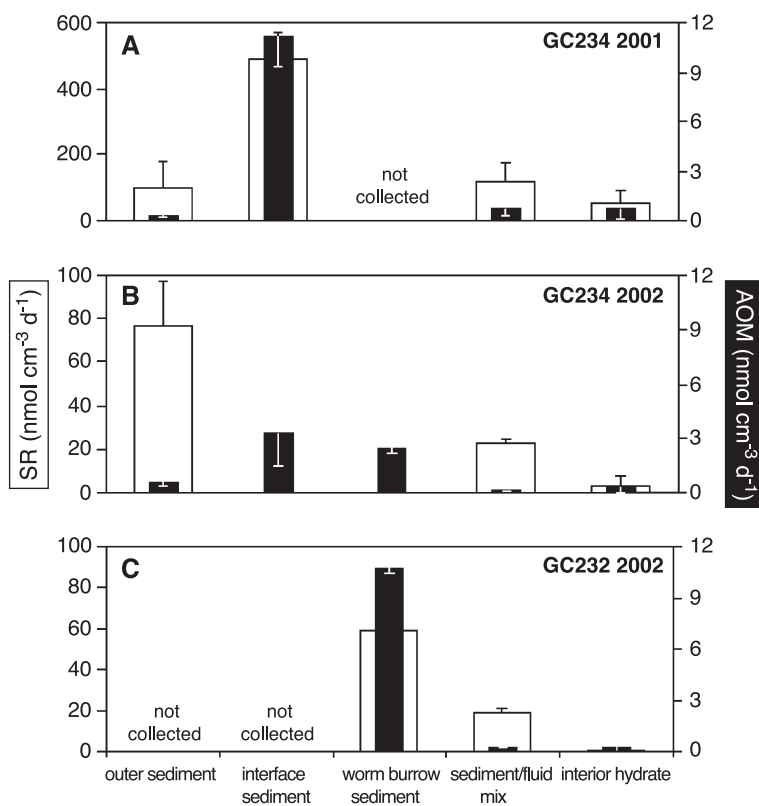


Fig. 4. Rates of AOM and SR in hydrate material collected from Gulf of Mexico hydrate sites in 2001 and 2002. SR rates (white columns) are plotted on the left axes; black error bars are one standard deviation of the mean. AOM rates (black columns) are plotted on the right axes; white error bars represent one standard deviation of the mean values. Note the changes in scale for the different axes. Sample types are shown on the x-axis. (A) Rates determined in slurried material (see text) from GC234 in 2001; (B) rates from GC234 material in 2002; (C) rates from GC232 material in 2002. Note that SR rates in B and C were determined in non-slurried material while AOM rates were determined in slurried samples (see text).

2) suggesting differences in the abundance of AOM-related microorganisms or in the cell-specific rates of microbial activity.

3.4. Sulfate reduction rates

Sulfate-reduction was observed in all hydrate subsamples (Table 2, Fig. 4). The spatial distribution of SR was comparable to that of AOM with the highest rates occurring in hydrate-drape sediments but SR rates were usually an order of magnitude higher than AOM rates. High variability in SR rates was probably also related to variation in the abundance of sulfate reducing microorganisms in the samples. In the 2001 GC234 slurry experiments, the highest rates of SR were observed in the IS ($489.1 \text{ nmol cm}^{-3} \text{ day}^{-1}$). The OS and MIX material exhibited similar SR rates between 100 and $118 \text{ nmol cm}^{-3} \text{ day}^{-1}$ while the lowest rates were observed in the IN ($54.7 \text{ nmol cm}^{-3} \text{ day}^{-1}$). In the 2002 non-slurry experiments at both sites, the highest SR rates were observed in the hydrate-drape sediments (76 and $59 \text{ nmol cm}^{-3} \text{ day}^{-1}$ in OS and WB, respectively; Fig. 4) while lower rates were observed in the sediment-poor hydrate layers ($\sim 20 \text{ nmol cm}^{-3} \text{ day}^{-1}$ in MIX and $\leq 3.2 \text{ nmol cm}^{-3} \text{ day}^{-1}$ in IN).

4. Discussion

These data provide the first evidence of anaerobic oxidation of methane and sulfate reduction in gas hydrate materials and in hydrate-drape sediments (Table 2, Fig. 4). Our data clearly illustrate that active microbial populations are present in all layers of the hydrate (Fig. 1), particularly at the boundary between hydrate and the overlying hydrate-drape sediments. However, our data cannot distinguish whether the active microbial communities inside gas hydrate reside within the hydrate structure or within brine inclusions or sediment trapped within the hydrate lattice.

Rates of AOM and SR in hydrate-drape sediment ($0.3\text{--}11.2$ and $59\text{--}490 \text{ nmol cm}^{-3} \text{ day}^{-1}$, respectively) are lower than rates in associated sediments at these same sites in the Gulf (by a factor of 10 to 100, Joye et al., 2004). The AOM rates in hydrate-drape sediments are comparable to rates of AOM in other

marine sediments (Iversen and Jørgensen, 1985; Alperin and Reeburgh, 1984; Hoehler et al., 1994) but are lower than rates observed in methane-rich seep sediments (Bussman et al., 1999; Aharon and Fu, 2000; Boetius et al., 2000; Arvidson et al., submitted for publication; Joye et al., 2004). Hydrate-drape sediments may experience greater frequency of disturbance as nearby sediments and this might influence the accumulation of active microbial biomass at the hydrate–sediment interface. Fluctuating sediment distribution and varying geochemical conditions result from the dynamic nature of the hydrates themselves: time-lapse photographic evidence demonstrates growth and retreat of hydrates, sloughing off of draping sediment, as well as the variable distribution and activity of vacuolate sulfur bacteria and “ice worms” on the hydrate surface (MacDonald, 1994, 2003). However, nutrient and bioactive trace metal availability probably also play an important role in controlling microbial distribution and activity within and adjacent to gas hydrates. Understanding the environmental controls on microbial distribution and activity in hydrates and adjacent sediments requires further study.

Previously, comparison of the molecular isotopic composition of solid hydrate with that of vent gas showed isotopic enrichment of ^{13}C in hydrate-bound CH_4 , suggestive of microbial consumption of CH_4 within the hydrate (Sassen et al., 1999). We observed depletion in the percent of CH_4 , relative to other hydrocarbons, in outer layers of the hydrate, relative to inner layers (at GC234), which could result in situ from CH_4 oxidation (as suggested by Sassen et al., 1998, 1999). Furthermore, deviation of the hydrate melt fluid from expected SO_4/Cl ratio (assuming no bias in the relative exclusion of these ions from the hydrate lattices during formation) is suggestive of the microbial consumption of SO_4^{2-} in these environments under in situ conditions.

Spatial patterns of CH_4 and SO_4^{2-} consumption are evident between the hydrate layers, with maximum rates of both processes occurring at the interface of sediment and hydrate (Table 2, Fig. 4). Microorganisms living at the edge of methane ice have simultaneous access to the source of dissolved CH_4 as well as to oxidants in the hydrate-drape sediment, which could enhance both AOM and SR rates. High flux rates of oxidants (SO_4^{2-}) and reductants (methane,

higher alkanes and oil) may result from the dissolution of hydrate and release of reductants across the hydrate boundary as well as the dynamic turnover of the oxidant pool at the hydrate surface via biological (i.e. sulfide oxidizing bacteria, “ice worms”; Nelson et al., 1986; Fisher et al., 2000; Joye et al., 2004) and abiological (i.e. bubble-induced mixing; O’Hara et al., 1995) mixing. Microbial activity at the sediment/hydrate boundary thus creates a living interface in the hydrate ecosystem, potentially altering the flux of methane from these structures into the surrounding sediments and the over-lying water column (Suess et al., 1999).

The normalized rates presented here (particularly the AOM rates) are likely to be conservative estimates of in situ rates. Our experiments were conducted at lower CH₄ concentrations (≤ 1 mM CH₄ compared to over 70 mM CH₄ under in situ conditions (5–7 MPa, 7 °C)) and much lower pressures (0.1 MPa) than experienced in situ (5–7 MPa). While slurring of sediment may increase activity, our data are nonetheless likely reflective of the general patterns of activity occurring in situ because the same spatial distribution of activity was observed in slurries and in whole sediment incubations. Although a similar spatial distribution of AOM and SR rates was observed in all samples, rates of SR were typically two to three orders of magnitude higher than the corresponding AOM rates (Table 2). In the slurry experiments, this offset can be explained in part by sulfate enrichment from the slurring process. The lack of stoichiometric (i.e., 1:1) balance between the two processes suggests that only a fraction of sulfate reduction is coupled directly to AOM. This loose coupling between SR and AOM is quite different from the efficient (1:1) coupling observed in other systems (Nauhaus et al., 2002; Michaelis et al., 2002). However, in the GOM hydrocarbon basin, in addition to methane, oil and other hydrocarbons are abundant, and these other C substrates serve as additional reductants (or substrates) to fuel sulfate reduction (Zengler et al., 1999; Heider et al., 1999; Joye et al., 2004).

The rates of both AOM and SR measured in material from the interior hydrate exhibited significant variability in replicate samples (Table 2, Fig. 4). The most likely explanation for this variability is environmental heterogeneity. It is possible and likely

that the separate samples of hydrate material collected during multiple dives were quite different with respect to each other. These differences arise from differing amounts of entrapped sediment particles or seawater, which may influence the distribution of microorganisms, the concentrations of substrates (especially) sulfate and thus may influence the measured activity. While activity of both AOM and SR are evident in material from the hydrate interior, rates of these processes on a volumetric basis are lower than those observed in the sediment-rich layers (Table 2, Fig. 4). The hydrate interior represents a very different physical and geochemical environment with observed lower biomass content than outer sediments (10^7 cells cm⁻³ in hydrate versus 10^9 cells cm⁻³ in hydrate-drape sediments). If process (AOM and SR) activities are corrected for microbial numbers per volume of material, the cell-specific activities are comparable between the hydrate-drape sediments and the material from the interior hydrate. This indicates that the microorganisms residing in the interior region hydrate have similar metabolic capabilities to microorganisms in the surrounding sediments. Microscopic evaluation of the hydrate material types revealed that microorganisms from the interior of the hydrate had similar morphologies (rod-shaped cells dominating) to microorganisms in hydrate-draping sediments (Fig. 3), which may suggest that these microorganisms are derived from trapped or migrating pore fluids or sediment grains.

The distribution and activity of microorganism in hydrates may be determined by similar factors that drive the distribution of microbes in sea ice. In sea ice, microbial communities are concentrated in pockets of brine fluid within the ice matrix (Eicken, 1992). Sea ice microbial communities may also create biofilms of “extracellular polymeric substances,” which could alter the physiochemical structure of their niche to promote continued growth (Thomas and Dieckmann, 2002). Microorganisms residing within the interior hydrates may experience similar conditions and may exploit similar adaptations, e.g., focusing populations in certain regions and/or excreting mucous. Furthermore, as hydrates form, small channels or pockets of brine solution (a concentrated mixture containing salts, nutrients, and dissolved gases) may develop and sediments and their associated microbial popula-

tions, may be trapped within the frozen hydrate (Bohrmann et al., 1998). In such zones, microbes could survive and even proliferate. The inclusion of sediment particles in the hydrate matrices may also offer interfacial oasis for microbial life. These hypothetical habitats may represent unexpected niches for novel microorganisms, although microscopic evaluation suggests that microorganisms from interior hydrate material are morphologically similar to those observed in the outer sediments. However, a difference between hydrates and other ice-structures (sea ice, glaciers, permafrost) is that hydrate ice contains an abundance of methane. This methane, if bioavailable, provides a powerful fuel for microbes and the availability of dissolved methane, oxidant and nutrients is likely higher at the interface between the hydrate and bottom sediment/water environment, making this the most microbially active portion of the hydrate environment.

The evidence of microbial activity in samples from the interior of a methane hydrate further illustrates the extreme and remote reaches of microbial life here on Earth. Further research—such as *in vitro* pressure experiments and molecular biological quantification and identification of microbial communities—in these systems is needed to evaluate the range and dynamics of microbial activity. Investigating the successful ecological strategies of hydrate-bound microbial life may lead to broader understanding of geomicrobiological interactions at life's "extremes." Detection of microbial life within frozen, submarine gas hydrates should encourage continued study of life in other icy environments here on Earth (i.e. permafrost, glaciers, accretion ice; Priscu et al., 1999, 2002), as these data will further our ability to evaluate such habitats as a proxies for life in ice on other planets.

Acknowledgements

We thank members of the LExEn 2001 and 2002 scientific parties for assistance on board ship, especially Matthew Erickson, who provided help with laboratory analyses. We thank the crews of the R/V Seward Johnson I and II and the pilots and crew of the deep submergence vehicle Johnson Sea Link for assistance with sample collection. Two anonymous reviewers provided valuable comments that improved

our manuscript. Submersible operations support was provided by the National Undersea Research Program and the US Department of Energy. Support for this work was provided by the National Science Foundation (OCE-0085549), the American Chemical Society (PRF-36834-AC2), the German Federal Ministry for Education and Research (03G0554A) and the Max Planck Society. Additional support was provided by a Barry Goldwater scholarship and a University of Georgia recruiting fellowship (BNO) and by a sabbatical fellowship (SBJ) by the Hanse Institute for Advanced Study, Delmenhorst, Germany. This is publication number 19 of the GEOTECHNOLOGIEN program of BMBF and DFG. [LW]

References

- Aharon, P., Fu, B., 2000. Microbial sulfate reduction rates and sulfur and oxygen isotope fractionations at oil and gas seeps in deepwater Gulf of Mexico. *Geochim. Cosmochim. Acta* 64, 233–246.
- Alperin, M.J., Reeburgh, W.S., 1984. Geochemical observations supporting anaerobic methane oxidation. In: Crawford, R., Hanson, R. (Eds.), *Microbial Growth on C₁ Compounds*. Amer. Soc. Microbiol. Press, Washington, DC, pp. 282–289.
- Arvidson, R., Morse, J.W., Joye, S.B., submitted for publication. The sedimentary biogeochemistry of Gulf of Mexico cold seeps. *Mar. Chem.* (in review).
- Boetius, A., Ravensschlag, K., Shubert, C.J., Rickert, D., Widdel, F., Gieseke, A., Amann, R., Jorgensen, B.B., Witte, U., Pfannkuche, O., 2000. Microscopic identification of a microbial consortium apparently mediating anaerobic methane oxidation above marine gas hydrates. *Nature* 407, 623–626.
- Bohrmann, G., Greinert, J., Suess, E., Torres, M., 1998. Authigenic carbonates from the Cascadia subduction zone and their relation to gas hydrate stability. *Geology* 26, 647–650.
- Brooks, J.M., Kennicutt III, M.C., Fay, R.R., McDonald, T.J., Sassen, R., 1984. Thermogenic gas hydrates in the Gulf of Mexico. *Science* 223, 696–698.
- Brooks, J.M., Field, M.E., Kennicutt III, M.C., 1991. Observations of gas hydrates in marine sediments, offshore northern California. *Mar. Geol.* 96, 103–109.
- Bussman, I., Dando, P.R., Niven, S.J., Suess, E., 1999. Groundwater seepage in the marine environment: role for mass flux and bacterial activity. *Mar. Ecol., Prog. Ser.* 178, 169–177.
- Canfield, D.E., Raiswell, R., Westrich, J.T., Reaves, C.M., Berner, R.A., 1986. The use of chromium reduction in the analysis of reduced inorganic sulfur in sediments and shales. *Chem. Geol.* 54, 149–155.
- Collett, T.S., Kuuskraa, V.A., 1998. Hydrates contain vast store of world gas resources. *Oil Gas J.* 96 (19), 90–95.
- Dickens, G.R., 2001. The potential volume of oceanic methane

- hydrates with variable external conditions. *Org. Geochem.* 32, 1179–1193.
- Dickens, G.R., O'Neil, J.R., Rea, D.K., Owen, R.M., 1995. Dissociation of oceanic methane hydrate as a cause of the carbon isotope excursion at the end of the Paleocene. *Paleoceanography* 10 (6), 965–971.
- Eicken, H., 1992. The role of sea ice in structuring Antarctic ecosystems. *Polar Biol.* 12, 3–13.
- Fisher, C.R., MacDonald, I.R., Sassen, R., Young, C.M., Macko, S.A., Hourdez, S., Carney, R.S., Joye, S.B., McMullin, E., 2000. Methane ice worms: *Hesiocoecca methanicola* colonizing fossil fuel reserves. *Naturwissenschaften* 87, 184–187.
- Fossing, H., Jørgensen, B.B., 1989. Measurement of bacterial sulfate reduction in sediments: evaluation of a single-step chromium reduction method. *Biogeochemistry* 8, 205–222.
- Ginsburg, G.R., Suseynov, R., Dadashev, A., Ivanova, G., Kazantsev, S., Solovyev, V., Telepnev, E., Askeri-Nasirov, R., Yesikov, A., 1992. Gas hydrates of the southern Caspian Sea. *Int. Geol. Rev.* 34 (8), 765–782.
- Ginsburg, G.D., Milkov, A.V., Soloviev, V.A., Egorov, A.V., Cherkashev, G.A., Vogt, P.R., Crane, K., Lorensen, T.D., Khutorskoy, M.D., 1999. Gas hydrate accumulation at the Haakon Mosby mud volcano. *Geo Mar. Lett.* 19 (1/2), 57–67.
- Heider, J., Spormann, A.M., Beller, H.R., Widdel, F., 1999. Anaerobic bacterial metabolism of hydrocarbons. *FEMS Microbiol. Rev.* 22, 459–473.
- Hesselbo, S.P., Gröcke, D.R., Jenkyns, H.C., Bjerrum, C.J., Farrimond, P., Morgans Bell, H.S., Green, O.R., 2000. Massive dissociation of gas hydrate during a Jurassic oceanic anoxic event. *Nature* 406, 392–395.
- Hinrichs, K.-U., Boetius, A., 2002. The anaerobic oxidation of methane: new insights in microbial ecology and biogeochemistry. In: Wefer, G., Billett, D., Hebbeln, D., Jørgensen, B.B., Schlüter, M., van Weering, T.C.E. (Eds.), *Ocean Margin Systems*. Springer-Verlag, Berlin, pp. 457–477.
- Hobbie, J.E., Daley, R.J., Jasper, S., 1977. Use of nucleopore filters for counting bacteria for fluorescence microscopy. *Appl. Environ. Microbiol.* 33, 1225–1228.
- Hoehler, T.M., Alperin, M.J., Albert, D.B., Martens, C.S., 1994. Field and laboratory studies of methane oxidation in an anoxic marine sediment—evidence for a methanogen-sulfate reducer consortium. *Glob. Biogeochem. Cycles* 8, 451–463.
- Hoehler, T.M., Borowski, W.S., Alperin, M.J., Rodriguez, N.M., Paull, C.K., 2000. Model, stable isotope, and radiotracer characterization of anaerobic methane oxidation in gas hydrate-bearing sediments of the Blake Ridge. In: Paull, C.K., Matsumoto, R., Wallace, P.J., Dillon, W.P. (Eds.), *Proceedings of the Ocean Drilling Program. Scientific Results*, vol. 164. Ocean Drilling Program, College Station, TX, pp. 79–85.
- Iversen, N., Jørgensen, B.B., 1985. Anaerobic methane oxidation rates at the sulfate-methane transition in marine sediments from Kattegat and Skagerrak (Denmark). *Limnol. Oceanogr.* 30, 944–955.
- Joye, S.B., Connell, T., Miller, L.G., Oremland, R.S., Jellison, R., 1999. Oxidation of ammonia and methane in an alkaline, saline lake. *Limnol. Oceanogr.* 44, 178–188.
- Joye, S.B., Orcutt, B.N., Boetius, A., Montoya, J.P., Schulz, H.N., Erickson, M.J., Lugo, S.K., submitted for publication. Sediment signatures of the anaerobic oxidation of methane and sulfate reduction at Gulf of Mexico cold seeps. *Chem. Geol.* (in review).
- Kennett, J.P., Cannariato, K.G., Hendy, I.L., Behl, R.J., 2000. Carbon isotopic evidence for methane hydrate instability during quaternary interstadials. *Science* 288, 128–133.
- Kennicutt, M.C., Brooks, J.M., Denoux, G.J., 1988. Leakage of deep reservoir petroleum to the near surface of the Gulf of Mexico continental slope. *Mar. Chem.* 24, 39–59.
- Kvenvolden, K.A., 1988. Methane hydrates and global change. *Glob. Biogeochem. Cycles* 2 (3), 221–229.
- Kvenvolden, K.A., 1993. Gas hydrates—geological perspective and global change. *Rev. Geophys.* 31, 173–187.
- Lanoil, B.D., Sassen, R., La Duc, M.T., Sweet, S.T., Nealson, K.H., 2001. Bacteria and Archaea physically associated with Gulf of Mexico gas hydrates. *Appl. Environ. Microbiol.* 67 (11), 5143–5153.
- MacDonald, I.R., Boland, Baker, J.S., Brooks, J.M., Kennicutt, R.R., Bidigare, R.R., 1989. Gulf of Mexico chemosynthetic communities: II. Spatial distribution of seep organisms and hydrocarbons at Bush Hill. *Mar. Biol.* 101, 235–247.
- MacDonald, I.R., Guinasso Jr., N.L., Sassen, R., Brooks, J.M., Lee, L., Scott, K.T., 1994. Gas hydrate that breaches the sea-floor on the continental slope of the Gulf of Mexico. *Geology* 22, 699–702.
- MacDonald, I.R., Sager, W.W., Peccini, M.B., 2003. Gas hydrate and chemosynthetic biota in mounded bathymetry at mid-slope hydrocarbon seeps: Northern Gulf of Mexico. *Mar. Geol.* 198, 133–158.
- Michaelis, W., Seifert, R., Nauhaus, K., Treude, T., Thiel, V., Blumenberg, M., Knittel, K., Gieseke, A., Peterknecht, K., Pape, T., Boetius, A., Amann, R., Jørgensen, B.B., Widdel, F., Peckmann, J., Pimenkov, N., Gulin, M.B., 2002. Microbial reefs in the black sea fueled by anaerobic methane oxidation. *Science* 297, 1013–1015.
- Nauhaus, K., Boetius, A., Krüger, M., Widdel, F., 2002. In vitro demonstration of anaerobic oxidation of methane coupled to sulfate reduction from a marine gas hydrate area. *Environ. Microbiol.* 4, 296–305.
- Nelson, D.C., Revsbech, N.P., Jørgensen, B.B., 1986. Microoxic–anoxic niche of *Beggiatoa* spp.: microelectrode survey of marine and freshwater strains. *Appl. Environ. Microbiol.* 52, 161–168.
- Norris, R.D., Röhl, U., 1999. Carbon cycling and chronology of climate warming during the Paleocene/Eocene transition. *Nature* 401, 775–778.
- O'Hara, S.C.M., Dando, P.R., Schuster, U., Bennis, A., Boyle, J.D., Chiu, F.T.W., Hatherell, T.V.J., Niven, S.J., Taylor, L.J., 1995. Gas seep induced interstitial water circulation: observations and environmental implications. *Cont. Shelf Res.* 15, 931–948.
- Orphan, V.J., House, C.H., Hinrichs, K.-U., McKeegan, K.D., Delong, E.F., 2001. Methane-consuming archaea revealed by directly coupled isotopic and phylogenetic analysis. *Science* 293, 484–487.
- Orphan, V.J., House, C.H., Hinrichs, K.-U., McKeegan, K.D., Delong, E.F., 2002. Multiple archaeal groups mediate methane

- oxidation in anoxic cold seep sediments. *Proc. Natl. Acad. Sci. U. S. A.* 99, 7663–7668.
- Priscu, J.C., Adams, E.E., Lyons, W.B., Voytek, M.A., Mogk, D.W., Brown, R.L., McKay, C.P., Takas, C.D., Welch, K.A., Wolf, C.F., Kirshtein, J.D., Avci, R., 1999. Geomicrobiology of subglacial ice above Lake Vostok, Antarctica. *Science* 286, 2141–2144.
- Reeburgh, W.S., 1980. Anaerobic methane oxidation: rate depth distributions in Skan Bay sediments. *Earth Planet. Sci. Lett.* 47, 345–352.
- Reeburgh, W.S., 1996. “Soft Spots” in the global methane budget. In: Lidstrom, M.E., Tabita, F.R. (Eds.), *Microbial Growth on C₁ Compounds*. Kluwer Academic Publishing, Dordrecht, The Netherlands, pp. 334–342.
- Reeburgh, W.S., Whalen, S.C., Alperin, M.J., 1993. The role of methyloxytrophs in the global methane budget. In: Murrell, J.C., Kelly, D.P. (Eds.), *Microbial Growth on C₁ Compounds*. Intercept, Andover, England, pp. 1–14.
- Sassen, R., MacDonald, I.R., 1994. Evidence of structure H hydrate, Gulf of Mexico continental slope. *Org. Geochem.* 23, 1029–1032.
- Sassen, R., MacDonald, I.R., Guinasso, N.J., Joye, S.B., Requejo, A.G., Sweet, S.T., Alcalá-Herrera, J., DeFreitas, D.A., Schink, D.R., 1998. Bacterial methane oxidation in sea-floor gas hydrate: significance to life in extreme environments. *Geology* 26 (9), 851–854.
- Sassen, R., Joye, S., Sweet, S.T., DeFreitas, D.A., Milkov, A.V., MacDonald, I.R., 1999. Thermogenic gas hydrates and hydrocarbon gases in complex chemosynthetic communities, Gulf of Mexico continental slope. *Org. Geochem.* 30, 485–497.
- Sloan, E.D., 1990. *Clathrate Hydrates of Natural Gases*. Marcel Dekker, New York.
- Suess, E., Torres, M.E., Bohrmann, G., Collier, R.W., Greinert, J., Linke, P., Rehder, G., Trehu, A., Wallmann, K., Winckler, G., Zuleger, E., 1999. Gas hydrate destabilization: enhanced dewatering, benthic material turnover and large methane plumes at the Cascadia convergent margin. *Earth Planet. Sci. Lett.* 170 (1–2), 1–15.
- Thomas, D.N., Dieckmann, G.S., 2002. Antarctic sea ice—a habitat for extremophiles. *Science* 295, 641–644.
- Valentine, D.L., Blanton, D.C., Reeburgh, W.S., Kastner, M., 2001. Water column methane oxidation adjacent to an area of active hydrate dissociation, Eel river Basin. *Geochim. Cosmochim. Acta* 65, 2633–2640.
- Whiticar, M.J., 1996. Isotope tracking of microbial methane formation and oxidation. In: Adams, D.D., Crill, P.M., Seitzinger, S.P. (Eds.), *Cycling of Reduced Gases in the Hydrosphere*, *Mitteilung (Communications)*, vol. 23. Internationalen Vereinigung für Theoretische und Angewandte Limnologie, E. Schweizerbart'sche Verlagsbuchhandlung (Nägele u. Obermiller), Stuttgart, Germany, pp. 39–54.
- Zengler, K., Richnow, H.H., Rossello-Mora, R., Michaelis, W., Widdel, F., 1999. Methane formation from long-chain alkanes by anaerobic microorganisms. *Nature* 40, 266–269.